

Superconducting Tunnel Junction Detectors for Extreme Ultraviolet Applications

Christopher M. Wilson, Luigi Frunzio, and Daniel E. Prober

Abstract—We present measurements of superconducting tunnel junction (STJ) spectrometers optimized for extreme ultraviolet energies (EUV), between 20–200 eV. The high count rates demands of astronomical applications, such as solar flare studies, uniquely suit STJs as compared to other cryogenic spectrometers. We have simulated EUV measurements with the technique of multiphoton absorption using a pulsed UV laser as a light source. We have demonstrated an energy resolution of 2.15 eV, close to the requirements of the applications. This resolution is limited by amplifier noise. We present predictions of improved resolution based on new amplifier designs.

Index Terms—Extreme ultraviolet, spectroscopy, superconducting devices.

I. INTRODUCTION

CRYOGENIC spectrometers are maturing as a technology. After more than a decade of development, cryogenic spectrometers are beginning to enable new types of measurements. Spectrometers based on superconducting tunnel junctions (STJ) and transition edge sensors (TES) already been used in applications ranging from optical astronomy to x-ray microanalysis of biological and industrial materials [1], [2]. In this paper, we consider spectrometers optimized for a new application: extreme ultraviolet (EUV) astrophysics. As an example of this field, we can consider the study of solar flares. To understand the detailed physics of the solar flares, astronomers need to observe the emission spectrum of the flares as they evolve in time. Current observation techniques couple an imaging system without energy resolution with a separate spectrometer. The imaging system is used to find the eruption of a solar flare and then the spectrometer is trained on the flare. Unfortunately, with this technique, the spectrum of the flare in its earliest moments is lost. A detector that could combine imaging with energy resolution would solve this problem. In particular, the application requires spectrometers with an energy resolution of $\Delta E = 1\text{--}2$ eV full width at half maximum (FWHM) in the energy range $E_\gamma = 20\text{--}200$ eV, photon timing, and high photon count rates. The application only requires modest imaging capability. The field of view of each pixel only needs to be small enough such that the emission of a flare in that pixel is not overwhelmed

by the steady-state background. A focal-plane array of STJ detectors could meet all of these requirements. In addition, the high count rate requirement means that this application is particularly well suited to STJs versus other cryogenic spectrometers.

In this paper, we present preliminary measurements of STJs optimized for EUV applications. Directly testing these devices with EUV radiation would be both expensive and difficult. No common radioactive sources produce radiation in this energy range. In general, it can only be produced by synchrotrons or the discharge of highly ionized plasmas. In addition, it is difficult to couple the radiation from the source to the detectors. For these reasons we instead test our devices using the technique of multiphoton absorption. We use a pulsed N_2 laser to produce short bursts of UV photons. The photons are brought from room temperature to the STJ by a UV/optical fiber. Multiple photons from each burst are then absorbed by the detector. Since the duration of the bursts is much shorter than the important physical timescales of the STJ [3], the simultaneous absorption of photons simulates the absorption of a single high energy photon.

II. MEASUREMENTS

We use a lateral STJ geometry [4], in contrast with many other groups that use a vertical geometry [2]. We use a superconducting Ta absorber, with an energy gap $\Delta_{Ta} = 700 \mu\text{eV}$. The absorber is in good metallic contact with one electrode of an Al/Al-oxide/Al tunnel junction. (The tunnel junction area does not overlap the Ta absorber and the energy gap measured from $I\text{--}V$ curves is that of bulk Al, $\Delta_{Al} = 180 \mu\text{eV}$.) A photon absorbed in the Ta breaks Cooper pairs, creating excess quasiparticles. These quasiparticles diffuse until they reach the lower gap Al, where they scatter inelastically, becoming trapped. The trapped quasiparticles then tunnel across the barrier and our read out as an excess subgap current. This current is integrated to give a total detected charge, Q_γ , which is proportional to the incident photon energy, E_γ . The energy resolution of the STJ is fundamentally limited by the statistics of the various physical processes in the device, including quasiparticle creation and multiplication upon trapping. In the detectors measured here, we expect this limit to be

$$\Delta E_{stat} = 2.355\sqrt{0.45\varepsilon E_\gamma}, \quad (1)$$

where $\varepsilon = 1.7 \Delta_{Al}$ is the average energy required to create one quasiparticle and the factor 2.355 converts from one standard deviation to FWHM [5]. As we will show later, the energy resolution can also be affected by the noise of the read-out amplifier and other effects.

Manuscript received August 6, 2002. This work was supported in part by NASA Headquarters and NASA GSFC.

C. M. Wilson and D. E. Prober are with Yale University, Department of Applied Physics, New Haven, CT 06520 USA (e-mail: christopher.wilson@yale.edu; daniel.prober@yale.edu).

L. Frunzio was with Yale University and is now with Istituto di Cibernetica “Eduardo Caianiello” del Consiglio Nazionale delle Ricerche (C.N.R.), Via Campi Flegrei 34, I-80078 Pozzuoli (NA), Italy (e-mail: luigi.frunzio@yale.edu).

Digital Object Identifier 10.1109/TASC.2003.814170

We have measured the energy resolution of our STJs using a pulsed N₂ laser as a photon source. The N₂ laser emits intense bursts of light at 3.68 eV (337 nm). The length of each burst is about 4 ns. We can use the laser as a multiphoton source by adjusting the intensity such that more than one photon is absorbed during each burst. We believe multiphoton absorption can effectively simulate the response of the tunnel junction to a single higher energy photon. The photons are absorbed in a few nanoseconds but the excited quasiparticles diffuse to the junction over a period of a few microseconds, allowing the quasiparticle distribution to smooth before reaching the junction. In addition, the physical processes in the tunnel junction take place on microsecond timescales or longer and should effectively average over nanosecond variations in the absorption. In addition, since the device performance is limited by processes in the junction, multiphoton absorption should accurately simulate the energy resolution of the device [3], [6].

We have measured a number of STJs, all with 100 μm² tunnel junctions. The junctions are diamond shaped with a long axis of 20 μm and a short axis of 10 μm. In Fig. 1, we show histograms of the charge output of device 1 under laser illumination. Each count in the histograms represents the response of the detector to a single burst from the N₂ laser. The histograms shows a number of evenly spaced peaks, indicating that the number of photons absorbed varies from burst to burst. We expect this. We attenuate the laser's output at room temperature by 9 orders of magnitude, such that the probability of any one photon getting from the laser to the device is very small. If there is no correlation in the transmission of the photons, we expect the number of absorbed photons to follow a Poisson distribution. To test this hypothesis, we fit the histogram with a composite distribution:

$$P(Q) = \sum_{n=0}^{\infty} \left(\frac{\gamma^n e^{-\gamma}}{n!} \right) \frac{1}{\sqrt{2\pi\sigma^2}} \times \exp \left(-\frac{1}{2\sigma^2} (Q - (R \bullet nE_\gamma + Q_0))^2 \right) \quad (2)$$

where γ is the average number of photons absorbed, E_γ is the energy of a single photon, R is the responsivity, Q_0 is the charge offset, and σ is the standard deviation of the charge. The composite distribution is the sum of many identical Gaussian distributions evenly spaced in charge. The amplitude of each Gaussian is determined by a Poisson distribution. The energy resolution is calculated from the fit as $\Delta E = 2.355 \sigma/R$. The fits to the composite function are shown in Fig. 1 and we see that they agree quite well.

We can gain information by examining the structure of the histograms in more detail. First, we note that we get the best fit to the histograms if we assume the first peak represents laser pulses during which zero photons were absorbed. This is reasonable because we use a synchronization signal from the laser to trigger the data acquisition by the oscilloscope. Because of this, we actually expect to record some triggers during which no photon was absorbed. Second, we notice that the average charge of the zero-photon peak is not zero. This charge offset, Q_0 , is caused by phonons coupling from the substrate to the detector.

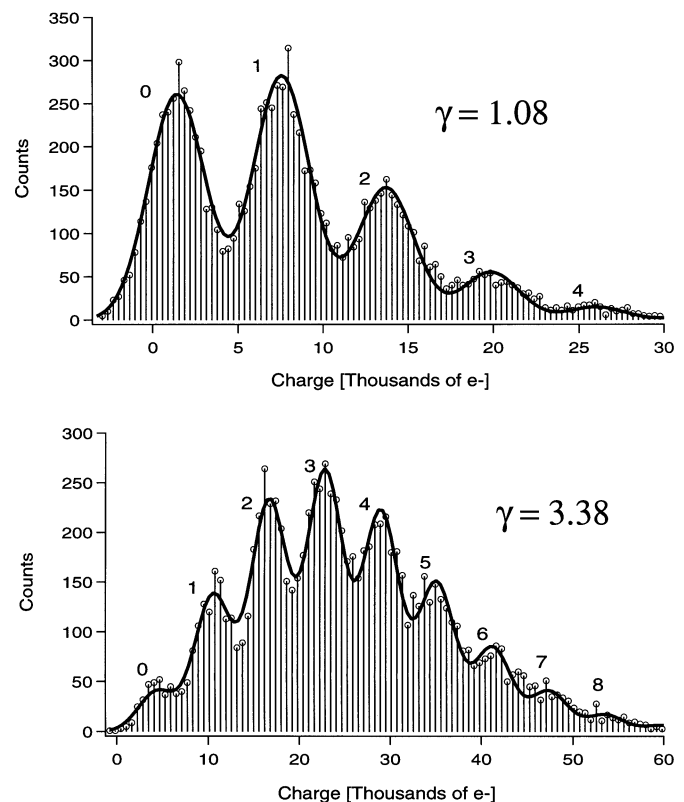


Fig. 1. Histograms of the charge output of device 1 in response to illumination with the N₂ laser. The histogram is fit with a composite function that distributes the counts according to a Poisson distribution. The two histograms represent the response for two different laser attenuations. Each graph is labeled with the average number of photons, γ , extracted from the fit. The peaks are labeled with the corresponding number of photons absorbed in the STJ.

As we have said earlier, the light emitted by the fiber onto the cold stage is dispersed over an area much larger than the detector. Thus, when the detector absorbs one photon, the substrate simultaneously absorbs $\sim 10^4$ photons. This energy is converted into phonons which can then couple to the detector and break pairs. Even though the coupling between the substrate and the detector is not very efficient, the number of quasiparticles created is significant because so much more energy is absorbed by the substrate than by the STJ.

We can distinguish this substrate signal from the absorber signal in the current pulses that we detect. In Fig. 2 we plot three waveforms which were recorded from a second device, device 2. Each waveform was produced by averaging pulses whose charge fell within a single peak of a multipeak histogram. In this case, the waveforms are the average of pulses from the 0, 1, and 2 photon peaks of a histogram with $\gamma = 0.80$ photons. The pulse from the 0 photon peak has a uniform decay with a very long time constant. We see that the 1 and 2 photon pulse shapes instead have a double exponential decay. They both have a fast component whose magnitude scales with the number of photons absorbed in the STJ. In addition, the time constant of the fast component matches the time constant measured when the device is excited with single photons from a Hg lamp. We also clearly see that the slow components from the 1 and 2 photon pulses are the same and they also match the decay of the 0 photon pulse. Therefore, we conclude that the slow component is independent

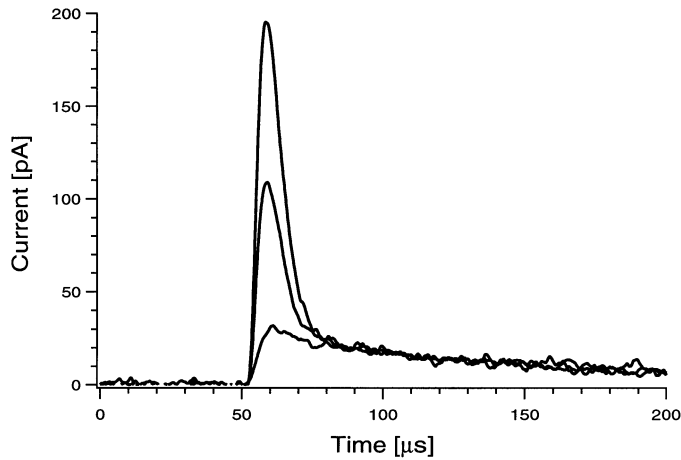


Fig. 2. Average current pulses from device 2. The pulse shapes are produced by averaging pulses whose charges are in one peak of a charge histogram (see Fig. 1). The pulses are, in order of increasing peak current, from the 0, 1, and 2 photon peaks of a histogram with $\gamma = 0.80$. We see the pulses have a fast component that scales with the number of photons and a slow component that is the same for all three.

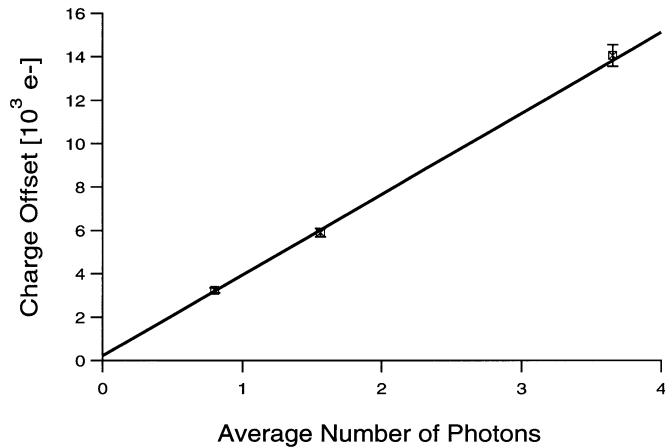


Fig. 3. Variation of the charge offset of the zero photon peak as a function of the average number of photons absorbed in the detector. The average number is varied by varying the room temperature attenuation of the laser. Error bars are shown, but are smaller than the symbols in some cases.

of the number of photons absorbed in the STJ and we infer that is due to excitation of the substrate.

We can exclude much of the substrate signal by windowing the pulses in time. Typically, we only use a $30 \mu\text{s}$ section of a pulse. Still, we expect the substrate effect to produce a charge offset in the histograms because some of the substrate signal is coincident in time with the absorber signal. As we have seen, this substrate signal is independent of the number of photons absorbed in the STJ. This implies all the peaks should be shifted to larger charge by the same average amount. The fits in Fig. 1 therefore assume that the peaks are equally spaced, but have an offset from zero. This assumption clearly fits the data. We do expect that the charge offset will vary with the attenuation of the laser intensity. If we decrease the attenuation, the substrate will absorb more energy during each pulse, ultimately breaking more pairs. Of course, decreasing the attenuation will also increase the average number of photons absorbed by the STJ. Fig. 3 shows the variation in the charge offset as a function of

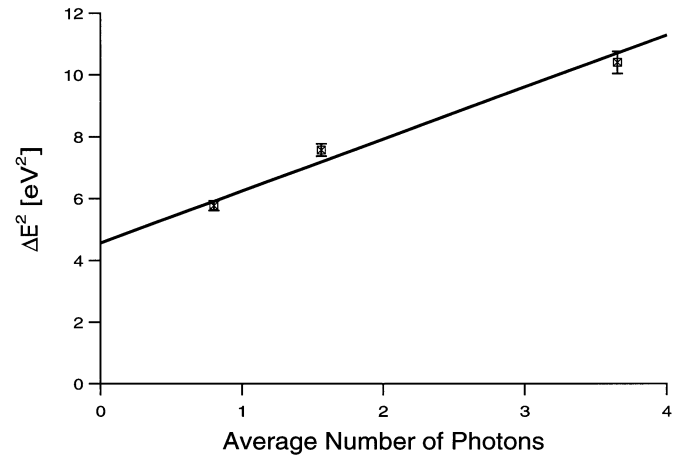


Fig. 4. The square of the energy resolution plotted against the average number of absorbed photons. The resolution extrapolated to zero photons gives the resolution not due to substrate noise.

the average number of photons absorbed. These offsets are obtained by fitting the histogram of charges, after windowing and filtering. (The average pulses in Fig. 2 were taken from the same three data sets.) We see that the offset varies linearly with the average number. We also see that the intercept is only slightly different from zero, meaning that if we turned the laser intensity to zero, there would be a negligible offset.

We also expect the substrate charge to degrade the energy resolution of the detector. This is because the amount of charge created by substrate phonons will vary from pulse to pulse. We can infer what part of the measured resolution is due to this substrate noise by studying how the resolution changes when we change the attenuation. To do this, we must make some assumptions. First, we assume that the substrate noise is independent and adds in quadrature with other noise sources. We can also guess that the variance of the substrate charge will be proportional to the average substrate charge. In Fig. 4 we show the square of the energy resolution as a function of the average number of photons absorbed in the STJ (which is proportional to the offset charge). We observe a number of things. First of all, the energy resolution clearly broadens as the average number of photons increases. It is also clear that for the lowest number, the energy width is not dominated by the substrate noise. If we fit a line to the data, we find that the substrate noise is about 1.3 eV per photon absorbed on average in the Ta and the remaining noise is about $2.14 \pm 0.07 \text{ eV}$.

We now want to understand what factors contribute to this 2.14 eV energy width. Electronic noise from the read-out amplifier is certainly one important contribution. We estimate the broadening due to the electronic noise in the following way. During a run, we can shutter the N_2 laser while still allowing it to electronically trigger the oscilloscope. We can then process these noise traces as if they were real photon pulses. If we do this, we get a histogram of charges with zero mean and some variance. Based on the responsivity measured from the multiphoton histogram, we can convert this charge noise to an energy resolution. We find an electronic noise resolution of 2.15 eV . Thus, within our measurement accuracy the resolution is fully accounted for by electronic noise and substrate noise.

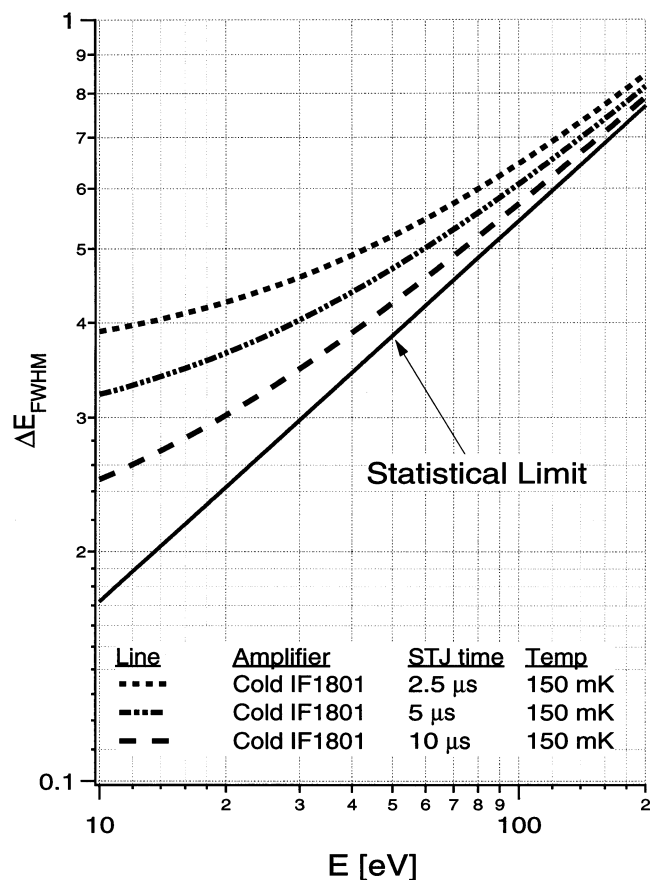


Fig. 5. Predicted energy resolution for improved amplifier. The plots are for the same amplifier with different STJ speeds. The trade-off between resolution and speed is most significant at lower energies. We assume the tunnel junction in all the STJ is $20 \mu\text{m}^2$.

III. FUTURE WORK

The demonstrated energy resolution of our STJs is already close to what is needed to be useful in EUV applications. Still, there are straightforward steps that can be taken to improve the energy resolution. First, the substrate can be masked from the UV laser to eliminate substrate effects. At the moment the electronic noise of our amplifier is dominated by the ac current noise of our active dc voltage bias circuit [7]. The active bias circuit was designed for x-ray detectors which need a much more stable bias than these EUV devices. We can, therefore, eliminate this noise by moving to a passive dc bias circuit. At our present operating temperature of $T = 210$ mK, the shot noise of the thermal bias current of the existing STJs should limit their resolution to about 1 eV. This noise can be reduced by making the

junctions smaller and reducing the operating temperature. Numerical simulations predict that the optimum junction size for EUV energies is about $20 \mu\text{m}^2$ [5]. This is factor of 5 smaller than the existing devices, implying that the shot noise would decrease by the square root of 5. In addition, if the magnitude of the bias current followed BCS predictions down to $T = 150$ mK, the shot noise would become completely negligible. After all of these improvements, we expect that the noise of the amplifier would be limited by the charge noise of the amplifier, which is the product of the input FET's voltage noise and the total capacitance at the input. The total capacitance includes both the capacitance of the FET and the capacitance of the leads running from the cold stage to room temperature. The capacitance our present measurement set-up is dominated by the lead capacitance. We can eliminate this in the future by moving the input FET inside the dewar, shortening the leads. We have recently tested the IF1801, made by InterFET, at cryogenic temperatures and found that it works well at cryogenic temperatures.

In Fig. 5, we make resolution predictions for STJ's read out by an amplifier based on a cold IF1801. We assume the junction area in each case is $20 \mu\text{m}^2$ and that $T = 150$ mK. We plot curves for STJs with three different tunnel times, implying different maximum count rates. We clearly see a trade-off between count rate and resolution, but it is most important only at lower energies. All three of these curves predict resolutions that exceed what is needed for EUV astronomy.

ACKNOWLEDGMENT

The authors would like to thank T. Stevenson and J. Davilla of NASA GSFC for useful discussions.

REFERENCES

- [1] B. Cabrera *et al.*, "Detection of single infrared, optical, and ultraviolet photons using superconducting transition edge sensors," *Appl. Phys. Lett.*, vol. 73, pp. 735–737, 1998.
- [2] N. Rando *et al.*, "S-Cam: A cryogenic camera for optical astronomy based on superconducting tunnel junctions," *IEEE Trans. Appl. Supercond.*, vol. 10, pp. 1617–1625, 2000.
- [3] S. Friedrich *et al.*, "Experimental quasiparticle dynamics in a superconducting, imaging x-ray spectrometer," *Appl. Phys. Lett.*, vol. 71, pp. 3901–3903, 1997.
- [4] C. M. Wilson *et al.*, "Optical/UV single-photon imaging spectrometers using superconducting tunnel junctions," *Nucl. Instrum. Meth. A*, vol. 444, pp. 449–452, 2000.
- [5] C. M. Wilson, "Optical/UV single-photon spectrometers using superconducting tunnel junctions," Ph.D. dissertation, Yale University, 2002.
- [6] K. Segall *et al.*, "Noise mechanisms in superconducting tunnel junction detectors," *Appl. Phys. Lett.*, vol. 76, pp. 3998–4000, 2000.
- [7] S. Friedrich *et al.*, "Single photon imaging x-ray spectrometer using low noise current preamplifiers with dc voltage bias," *IEEE Trans. Appl. Supercond.*, vol. 7, pp. 3383–3386, 1997.